Evaporative coolers for postharvest storage: where to best use them and how well do they work?

Thijs Defraeye [1] [*], Kanaha Shoji [1], Seraina Schudel [1], Daniel Onwude [1], Chandrima Shrivastava [1]

[1] Empa, Swiss Federal Laboratories for Materials Science and Technology, Laboratory for Biomimetic Membranes and Textiles, Lerchenfeldstrasse 5, CH-9014 St. Gallen, Switzerland

* *Corresponding author: thijs.defraeye@empa.ch (T. Defraeye) Empa, Swiss Federal Laboratories for Materials Science and Technology, Laboratory for Biomimetic Membranes and Textiles, Lerchenfeldstrasse 5, CH-9014 St. Gallen, Switzerland*

ABSTRACT

Passive evaporative coolers have a huge potential to help smallholder farmers to preserve their fresh fruit and vegetables longer after harvest. However, we still lack transparent information on where evaporative coolers perform sufficiently well to significantly extend the postharvest life of the fresh produce. Unsatisfactory evaporative cooler performance is a potential cause for farmers' limited adoption of this technology to reduce their food losses. We present easy-to-use tools that help to better scope regions with the best potential to deploy evaporative coolers. This information should help avoid installing evaporative coolers in areas with environmental conditions that incite insufficient cooling. Concretely, we developed design charts of the achievable temperature depression by evaporative cooling based on the local air temperature and humidity. We quantified for apple, banana, mango, and tomato the resulting additional days in postharvest life gained by storing the produce in an evaporative cooler. We present geographical maps of India, Nigeria, and the entire world that answer how much evaporative cooling can maximally decrease the produce temperature and extend postharvest life for banana fruit. We make these maps available online. We also quantify how well evaporative coolers perform with respect to reducing the temperature and how they should be sized. Our results facilitate installing evaporative coolers only in suitable regions where they successfully help to preserve food longer. Our data also show in which months the cooler can be operated with the best performance. We thereby avoid disillusions and loss of trust in the technology with smallholder farmers, policymakers, farmers, or farmer cooperatives. Further catalyzing the implementation of small-scale evaporative coolers can bring farmers significant gains in postharvest life, reduce food losses, and increase revenues.

1 Introduction

Evaporative cooling is considered a high-potential technological innovation that can help preserve fresh foods (GKI, 2017; Verploegen, 2021a). Evaporative coolers extract heat from the surrounding air and the fruit or vegetables in the cooler. This heat is the latent heat required to evaporate water. This water is stored in the porous material inside the cooler (e.g., charcoal). In evaporative coolers, we can reduce the product's temperature by typically 3-10 ºC and increase the relative humidity inside the cooler to up to 70%-100% (Defraeye et al., 2022). The reduced rate of food deterioration at lower temperatures and the reduced moisture loss help preserve the fruit or vegetables longer. Evaporative coolers work best in dry and warm regions.

These passive cooling systems are especially interesting for marginal or smallholder farmers and single-family households in remote, off-grid areas (Elansari et al., 2019; Teutsch and Kitinoja, 2019). If they are not part of a larger cooperative or farmer producer organization (FPO), these stakeholders do not always have access to active cooling or cannot afford it. Nevertheless, smallholder farmers produce a large amount of the world's food. Increased smallholder productivity is a large growth driver in future postharvest supply chains (Boettiger and Sanghvi, 2019; Goedde et al., 2019; Ricciardi et al., 2018). We, therefore, need affordable cooling solutions for smallholder farmers, such as evaporative cooling.

Several types of evaporative cooling systems are known. Examples are the zeer pot, sand and brick coolers, khus-mat coolers, and charcoal coolers. Despite their potential, these coolers are not widely deployed (Kanali et al., 2017). There are several reasons for this (Defraeye et al., 2022; Verploegen, 2021b). A main problem for smallholder farmers is one of scale. There are too many farmers and limited resources to have direct access to expertise, training, and sufficient capital to efficiently build and operate evaporative coolers. There is also a little economic incentive for companies to produce and disseminate such small-scale cooling facilities, despite the huge potential of this technology to help preserve food worldwide. In this case, one would need to interact with and train hundreds of farmers individually. Instead, companies that provide cooling solutions are more inclined to engage with larger clusters of farmers. Companies also prefer providing more controllable cooling solutions, such as micro-scale solar-powered cool rooms. The economic incentive is lacking for deploying evaporative coolers commercially, despite the huge potential of this technology to help preserve food worldwide. As a result of these hurdles, we notice that scientific funding, projects, and publications in this field are also limited. Only a few institutes actively research this topic. The scientific studies that were done in developing countries are mostly very applied. These countries include India, Cambodia, Laos, Kenya, and Nigeria (Ambuko et al., 2017; Anyanwu, 2004; Dadhich et al., 2008; Mujuka et al., 2021; Patel et al., 2021; Shitanda et al., 2011; Vanndy et al., 2008; Verploegen, 2021a).

As a result of this limited scientific and economic interest, the scientific basis of evaporative cooling devices is also rather limited (Rehman et al., 2020). An in-depth understanding of the underlying processes of how evaporative coolers work and perform for postharvest applications is rarely analyzed. Information on where and during which time of the year evaporative coolers perform best is also scarce (Verploegen, 2021c, 2021b). This lack of information for the stakeholders leaves key questions unanswered and hides the potential for optimization. Evaporative coolers should work to the best of their potential to preserve the fresh produce as long as necessary and for the farmers to keep their trust in these systems. Only then will farmers continue to use them over several seasons.

We use the theory of evaporative cooling to answer practical questions on evaporative cooling and its application. We quantify the maximal temperature reduction gained by evaporative cooling and visualize it into easy-to-use design charts for different stakeholders. Additionally, we determine the possible gains in postharvest life achieved through evaporative cooling. We focus on fruits, but the findings are also relevant to vegetables. We show on a world map in which location it makes the most sense to apply evaporative cooling. Here we show the maximal temperature reduction that can be achieved. Furthermore, we quantify how much fruit we can cool with a certain amount of water. Finally, we quantify the optimal thickness of the evaporative cooler walls and how this thickness affects the cooler performance.

2 Materials and Methods

The materials and methods are reported. We included several aspects directly in the supplementary material to condense the paper. Note that a detailed nomenclature is also included in the supplementary material.

2.1 **Wet-bulb temperature and temperature depression calculation**

There exist many empirical equations to directly calculate the wet-bulb temperature (θ_{wb} [°C] or T_{wb} [K]) from the dry-bulb temperature (θ_{db} [°C] or T_{db} [K]) and the relative humidity of the moist air (φ_a [%]) (Stull, 2011). However, we introduce an error in predicting the wet-bulb temperature with most empirical equations. This error can amount to 0.3-0.6 °C (supplementary material). Therefore, these 'direct' equations do not provide adequate sensitivity for estimating the design parameters of an evaporative cooler. In the present study, we calculate T_{wb} from T_{db} and φ_a using an iterative approach. This approach is based on the psychrometric constant γ [K^{-1}], which is often used to construct psychrometric tables (Allen et al., 2005; Jensen et al., 1990; Simões-Moreira, 1999). This approach converts the temperature depression (T_{wb}-T_{db}) into a vapor pressure deficit ($p_{v,sat}(T_{wb})$ - $p_{v,a}(T_{db})$) through well-established empirical coefficients for estimating vapor pressure from temperature and quantifying the latent energy (Sadeghi et al., 2013).

$$p_v \left\langle T_{db} \right\rangle - p_{v,sat} \left\langle T_{wb} \left\langle T_{db}, \varphi_a \right\rangle \right\rangle + \gamma \, P_{atm} (T_{db} - T_{wb}) = 0 \tag{1}$$

Here, p_v is the ambient vapor pressure so at the dry-bulb temperature [Pa], $p_{v,sat}$ is the saturated vapor pressure [Pa] at the wet-bulb temperature, and P_{atm} is the atmospheric pressure [Pa]. The angle brackets indicate here the main dependencies to other parameters. Here, γ is the psychrometric constant ($\gamma = c_{p,d} / (\varepsilon \cdot L_v^{ref}) \approx 0.65 \times 10^{-3}$ K^{-1}), derived from the latent heat of vaporization ($L_v^{ref} = 2.5$ MJ kg_l^{-1}), specific heat capacity of dry air at constant pressure ($c_{p,d} = 1006$ J kg_d^{-1} K^{-1}), and the ratio of molecular weights of water vapor and dry air ($\varepsilon = 0.622$ kg_v kg_d^{-1}). This value is not entirely constant but remains fairly constant up to wet-bulb temperatures of 40 °C (Simões-Moreira, 1999).

The saturated vapor pressure is derived as a function of temperature using Eq.(3), commonly referred to as Teten's equation (Allen et al., 1998).

$$p_{v,sat} = 610.8 \times \exp\left(\frac{17.27\theta}{\theta + 237.3} \right) \tag{2}$$

Here, θ represents the dry or wet-bulb temperature [°C], corresponding to ambient or saturated conditions. The ambient vapor pressure (p_v [Pa]) is calculated by computing $p_{v,sat}$ at T_{db} and multiplying this term by the relative humidity of the air (φ_a).

We solve Eq.(1) iteratively via the saturated vapor pressure $p_{v,sat}$ at wet-bulb temperature conditions to determine the wet-bulb temperature at different dry-bulb temperature and relative humidity values. The iterative process, underlying assumptions, initial guess, and margin of error are detailed in the supplementary material.

The maximal temperature depression achieved by evaporative cooling (ΔT_{ev} [K]) is calculated by subtracting wet-bulb temperature from dry-bulb temperature, using Eq.(3).

$$\Delta T_{ev} = T_{db} - T_{wb} \left\langle T_{db}, \varphi_a \right\rangle \tag{3}$$

2.2 **Calculating the maximal gain in postharvest life due to evaporative cooling**

The maximal gain in postharvest life of fruit (ΔPL_{fr} [days]) corresponding to this maximal temperature depression that can be achieved by evaporative cooling is evaluated at different combinations of T_{db} and φ_a. The maximal gain in postharvest life corresponds to the additional days gained by storing the fruit at wet-bulb temperature instead of ambient dry-bulb temperature conditions. These are the additional remaining days in a product's postharvest life when it is still marketable. We thus compare storing fruit inside an idealized evaporative cooler versus outside in the shade. This gain is thus the difference in postharvest life caused by the maximal temperature depression obtained from evaporative cooling. The postharvest life (PL_{fr} [days]) is calculated at each temperature using first-order kinetic models for respiration-driven quality decay for every fruit. We quantify the postharvest life for selected fruits, namely apple, banana, mango, and tomato. These models are detailed in the supplementary material. The maximal gain in postharvest life (ΔPL_{fr} [days]) is computed using Eq.(4).

$$\Delta PL_{fr} = PL_{fr}(T_{wb} \left\langle T_{db}, \varphi_a \right\rangle) - PL_{fr}(T_{db}) \tag{4}$$

Note that ΔPL_{fr} is the maximal gain in postharvest life achieved under ideal conditions. However, ΔPL_{fr} might be lower as the wet-bulb temperature is not always reached in evaporative cooling (Defraeye et al., 2022). Additionally,

the gain in postharvest life is only calculated based on the reduction in temperature due to evaporative cooling. Our current calculation does not account for the increase in postharvest life due to the reduced moisture loss due to increased relative humidity in the evaporative cooler. This reduced moisture loss in the evaporative cooler will also help to preserve the food longer.

2.3 Mapping the evaporative cooling potential for the world

We calculate and map the gain in postharvest life that evaporative cooling gives at every location in India and Nigeria for each month at a resolution of approximately 30 km. We also develop a similar map for the entire world for the four seasons, namely summer, autumn, winter, and spring. The details are given in the supplementary material. We combine the following data for calculating the wet-bulb temperature and the gain in postharvest life: local monthly climate data, psychometrics, information on postharvest life for each crop, and kinetic rate law modeling. As a benchmark, we calculate the postharvest life of fruit after harvest when stored under ambient conditions in the shade (T_{db}, φ_a). Then we calculate the postharvest life after harvest when stored in an idealized evaporative cooler, so at wet-bulb temperature conditions.

2.4 Calculating the potential of liquid water to cool fruit by evaporation

We know how much energy is extracted from the air and the horticultural products when 1 liter of water $(m_l = 1$ kg$)$ gets evaporated. This energy equals the latent heat needed for evaporating this 1 liter of water $(E_{lat} = m_l \cdot L_v^{ref})$. The energy is extracted from the air surrounding the evaporative cooler and the stored food. Here we assume idealized evaporative cooling, so just an energy conversion of sensible heat into latent heat in the air. The enthalpy of the air remains constant, so it is an isenthalpic process. For an ideal isenthalpic evaporative cooling process, the wet-bulb temperature is reached.

We calculate theoretically how many kilograms of fruit one liter of water can cool down from its initial temperature $(T_{ini}$ [K]$)$ to the wet-bulb temperature $(T_{wb}$ [K]$)$. T_{wb} is the lowest temperature that can be reached by evaporative cooling. For that, the following equation quantifies the energy needed to achieve this temperature reduction in the fruit by evaporative cooling $(E_{ec,fr}$ [J]$)$:

$$E_{ec,fr} = m_{fr} c_{p,fr} \left(T_{ini} - T_{wb} \right) \tag{5}$$

With m_{fr} the mass of fruit [kg], $c_{p,fr}$ the specific heat capacity of the fruit [J kg^{-1} K^{-1}], which is for apple fruit 3800 J kg^{-1}K^{-1}. Suppose we assume that all the energy needed to evaporate one liter of water is extracted from the fruit and not from the air. In that case, we have an ideally efficient evaporative cooling process. We can write the following equation, assuming that the fruit is initially equilibrated at the dry-bulb temperature of the environment:

$$E_{ec,fr} = m_{fr} c_{p,fr} \left(T_{db} - T_{wb} \right) = E_{lat} = m_l L_v^{ref} = 1kg \times 2'500'000 \frac{J}{kg} \tag{6}$$

$$m_{fr} = \frac{2'500'000}{c_{p,fr} \left(T_{db} - T_{wb} \right)} \tag{7}$$

This equation calculates the amount of fruit that can be cooled by evaporative cooling. This amount is a function of the ambient dry-bulb temperature and relative humidity, determining the wet-bulb temperature. The fruit's specific heat is the only fruit-dependent parameter in this equation. The heat of respiration was not factored in here. Highly respiring fruit will slightly change the heat balance during evaporative cooling and reduce the amount of fruit one liter of water can cool down.

2.5 Calculating the cooling power of an evaporative cooler

We quantify the cooling power or cooling capacity of an evaporative cooler. As an example, we take a charcoal cooler blanket we developed (Defraeye et al., 2022). We assume one square meter of a charcoal blanket $(A_{ec} = 1$ m$^2)$. The charcoal absorbed a certain amount of liquid water that can be evaporated $(m_{l,evap})$. This amount of water is estimated as:

$$m_{l,evap} = A_{ec} D_{ec} w_{PM,ec} = A_{ec} D_{ec} \left(1 - \phi_{0,bulk} \right) w_{PM} = A_{ec} D_{ec} \left(1 - \phi_{0,bulk} \right) X_{PM} w_s \tag{8}$$

5

Here, D_{ec} is the thickness of the evaporative cooler [m], $w_{PM,ec}$ is the bulk moisture content of the porous material (charcoal) in the evaporative cooler [kg m^{-3}], $\phi_{0,bulk}$ is the bulk porosity (or macroporosity) of the cooler, so the air space between the charcoal pieces, w_{PM} is the moisture content of the charcoal pieces (not saturated) [kg m^{-3}], X_{PM} is the dry-base moisture content of the charcoal [kg kg^{-1}], and w_s is the dry-base density of the charcoal pieces [kg m^{-3}].

The cooling capacity of the cooler, which holds this amount of water ($m_{l,evap}$), can be calculated based on the latent heat (2.5 MJ kg^{-1} of water) and the time interval over which the water is fully evaporated (Δt), so the evaporative cooling heat flow (Q_{evap} [W]). The average cooling power over this period (P_{ec} [W]) can be estimated as:

$$P_{ec} = Q_{evap} = L_v^{ref} G_{v,evap} = L_v^{ref} \frac{m_{l,evap} \left\langle A_{ec}, D_{ec}, \phi_{0,bulk}, X_{PM} \right\rangle}{\Delta t} \tag{9}$$

Note, however, that the evaporation rate ($G_{v,evap}$ [kg s^{-1}]) is not linear over this period. Thereby, the cooling capacity will also vary over time. With this equation, we only quantify the average cooling capacity. In addition, we cannot guarantee that this cooling capacity can be reached as this implies the amount of water can be evaporated in that amount of time. The time frames assume the airflow conditions are such that this amount can be evaporated.

Using the bulk moisture content and the thickness of the cooler, we get the cooling power as a function of the time interval and the cooler thickness:

$$P_{ec} = L_v^{ref} \frac{m_{v,evap} \left\langle D_{ec}, A_{ec}, \phi_{0,macro}, X_w \right\rangle}{\Delta t} = L_v^{ref} w_{PM,ec} A_{ec} \frac{D_{ec}}{\Delta t} \tag{10}$$

We quantify the average cooling power of this wall of an evaporative cooler based on our measurements of the charcoal properties and the charcoal cooler we developed previously (Defraeye et al., 2022). We assume a charcoal cooler with a bulk porosity of 61% ($\phi_{0,bulk}$), charcoal with a dry-base density of 442 kg m^{-3} (w_s), and a dry-base moisture content after wetting of about 20%. The moisture content of the porous material equals 88 kg m^{-3} (w_{PM}). These values give a bulk moisture content ($w_{PM,ec}$) of 34 kg m^{-3}.

2.6 Calculating the optimal thickness of an evaporative cooler

We should design the thickness of an evaporative cooler to reach the optimal cooling efficiency under the local airflow conditions at that specific location. The accessible surface area of the charcoal pieces for evaporation is relevant here when we assume air can flow through the porous structure. This implies a sufficient open porous stacking of the charcoal pieces and a permeable textile membrane. If the size or surface area for mass exchange is too low, air will be not be saturated. Then the air temperature will not reach the wet-bulb temperature. In the supplementary material, we calculate the optimal thickness of an evaporative cooler (D_{ec} [m]):

$$D_{ec} = \frac{U \cdot \rho_a \cdot \varepsilon}{CMTC \left\langle U \right\rangle \cdot P_{atm} \cdot A_{sf} \left\langle \phi_{0,bulk}, D_{cc} \right\rangle} \tag{11}$$

Here, A_{sf} is the surface area of the evaporative material for mass exchange per volume unit of the cooler [m^2 m^{-3}], U is the airspeed [m s^{-1}], ρ_a is the air density [kg m^{-3}], ε is the ratio of molecular weight of water and dry air [kg$_v$ kg$_d^{-1}$], CMTC is the convective mass transfer coefficient at the air-material interface [s m^{-1}], D_{cc} is the spherical piece size (e.g. charcoal) [m] and P_{atm} is the atmospheric pressure [Pa]. This simplified equation is only valid under steady-state conditions with no external heat exchange of the system with the environment, so an adiabatic system. The equation also assumes that the air becomes fully saturated after moving through the evaporative cooler. This case implies idealized evaporative cooling.

3   Results & Discussion

3.1   **What is the maximal temperature reduction we can get by evaporative cooling?**

We already know how much evaporative cooling can maximally reduce the air temperature. We can get the maximal temperature reduction (ΔT_{ev}) when the wet-bulb temperature is reached. The wet-bulb temperature is the theoretical lower limit to which we can cool down the air and the food products. This maximal temperature drop depends on the dry-bulb temperature and the relative humidity of the environment. In principle, psychometric charts contain this information (Figure 1). However, such a psychometrics-lookup exercise to determine the evaporative cooling temperature depression is tedious in the design phase. Consequently, it is time-consuming to look up the cooling potential for each month of the harvest season for different potential sites in a country.
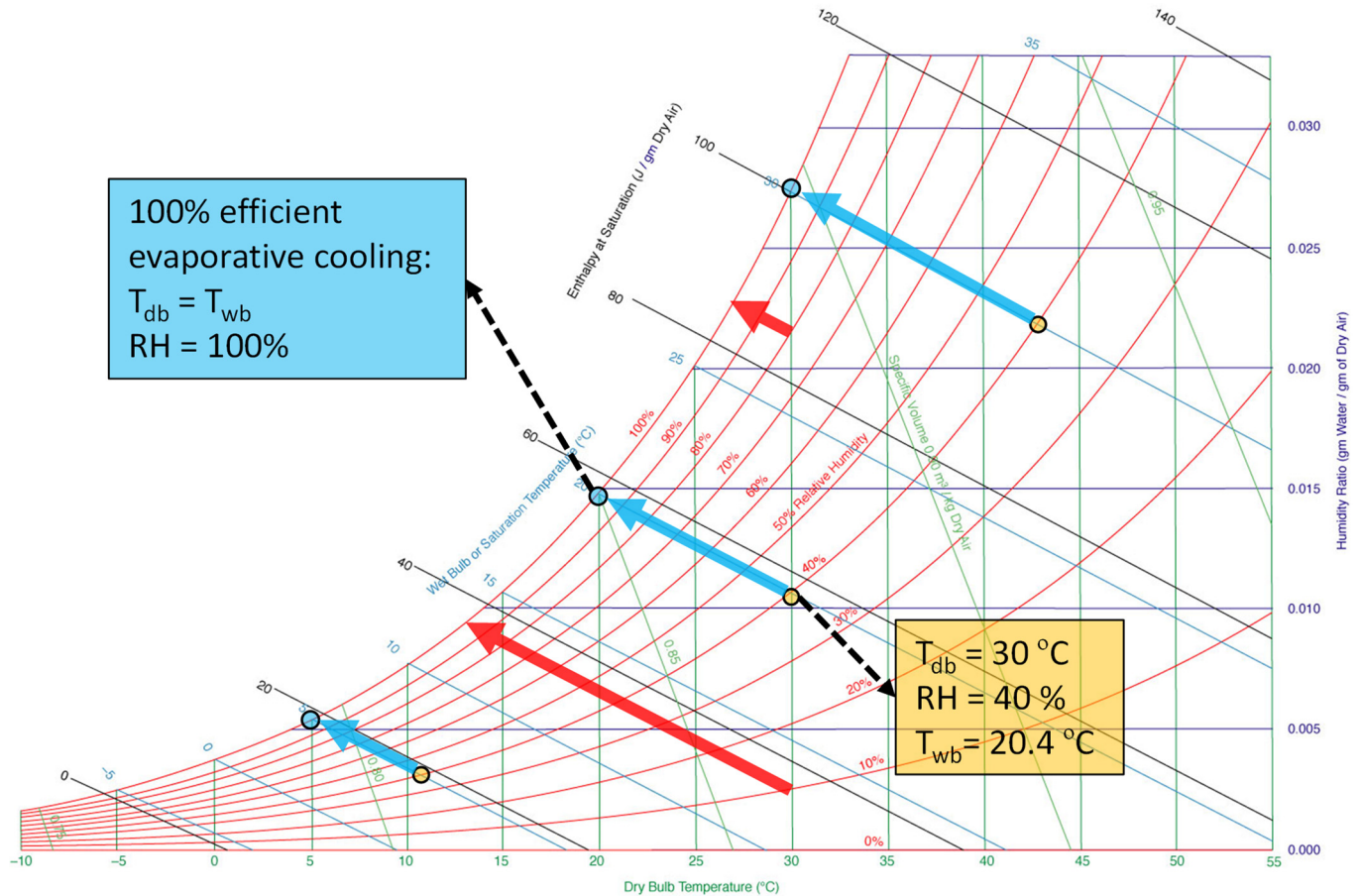
Figure 1. Psychrometric chart with an indication of the evaporative cooling process (adapted from (Ogawa, 2021)***). Blue arrows indicate the maximal temperature depression when starting at a relative humidity of 40% for several dry-bulb temperatures. Red arrows indicate the maximal temperature depression at a dry-bulb temperature of 30 °C starting at several relative humidities.***

Therefore, we present the following design charts for engineers developing evaporative coolers (Figure 2, Figure 3). They present the following parameters as a function of the ambient dry-bulb temperature and relative humidity:

- The wet-bulb temperature (T_{wb}), so the lowest temperature that can be reached by pure evaporative cooling (Figure 2a,c,e). This value is essential to determine for a certain food to which extent its ideal storage temperature can be reached.
- The temperature depression or drop invoked by evaporative cooling ($\Delta T_{ev} = T_{db}-T_{wb}$) (Figure 2b,d,f). This parameter is indicative of the gain in postharvest life that can be achieved. The Q_{10} value, namely the ratio between the rate constants of degradation reaction in the food, is typically 2-3 for fresh foods (Robertson,

2016). This implies that a decrease in temperature by 10 °C from the ambient, through evaporative cooling, typically doubles or triples the postharvest life of fruits and vegetables.

- The resulting gain in postharvest life compared to when the fruit is stored at ambient conditions, which is invoked by a specific temperature depression (Figure 3). We calculated this according to a kinetic rate law for the following species: apple, banana, mango, and tomato. The details of the quality model are given in the supplementary material.

From Figure 2, we can conclude that for a certain humidity, the warmer the region gets, the higher the maximal temperature depression becomes (Figure 2d). This increase is more pronounced in drier areas. The increase in temperature depression with increasing dry-bulb temperature at a constant humidity is almost linear (Figure 2d). The drier the region becomes for a certain dry-bulb temperature, the higher the maximal temperature depression becomes (Figure 2b). The increased temperature depression with decreasing relative humidity is also almost linear (Figure 2b). From Figure 2e, we see that in warm climates (T_{db} > 25°C), it will be unlikely to reach the ideal storage conditions for several fruits unless the air is very dry. The presented design charts (Figure 2 e,f) enable faster identification of the wet-bulb temperature and temperature depression than the traditional psychometric charts since they only depict the wet-bulb temperature.
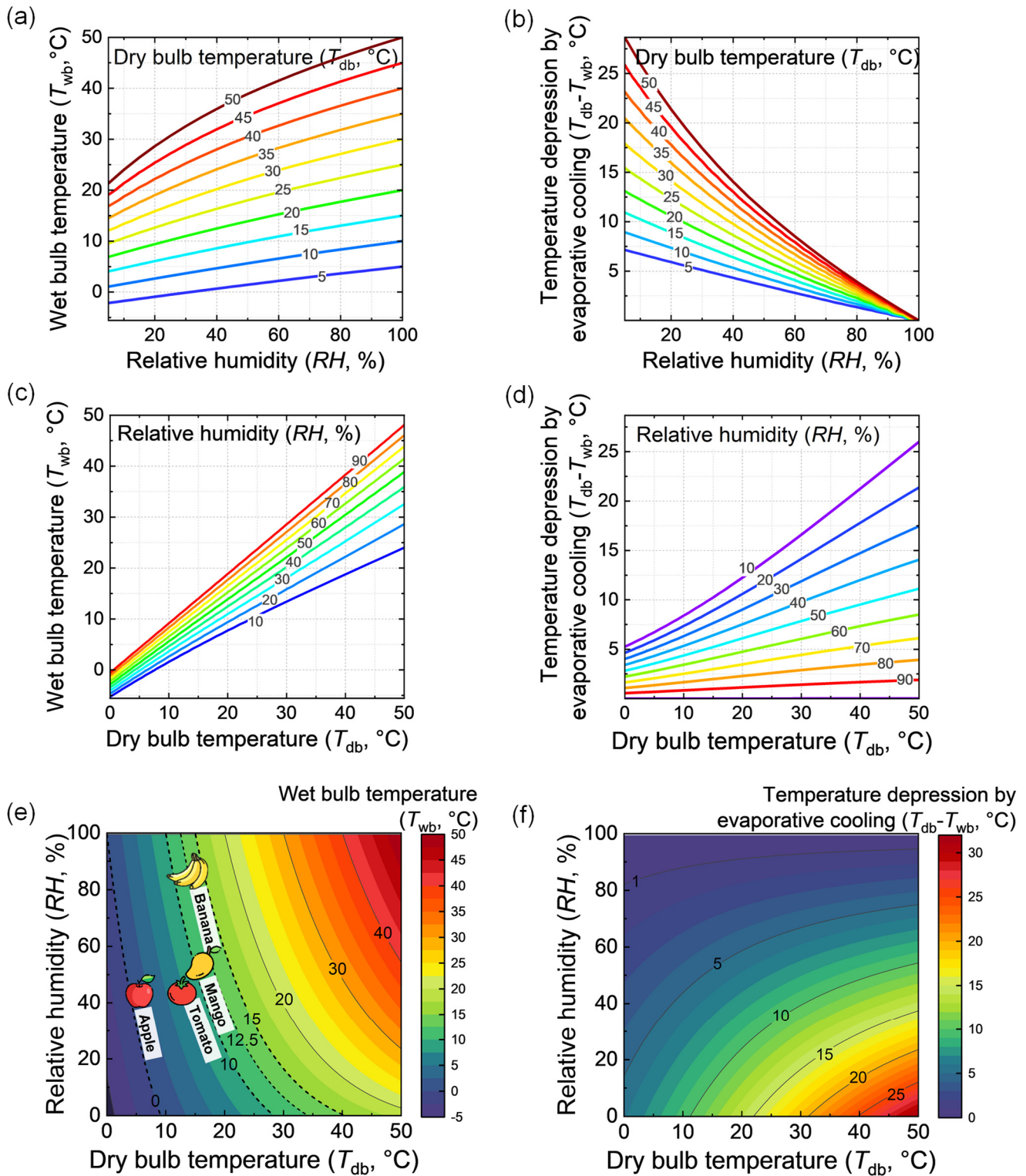
Figure 2 Design charts that show parameters as a function of dry-bulb temperature and relative humidity: (a,c,e) wet-bulb temperature, including an indication of optimal storage temperature conditions for several fruits (dotted lines in (e)); (b,d,f) maximal temperature depression invoked by evaporative cooling, namely when the wet-bulb temperature is reached. This image was created using resources from Flaticon.com.

Figure 3 shows that the temperature reduction induced by evaporative cooling can lead to several days of additional postharvest life. Here the gain in postharvest life implies the additional days gained by storing the fruit in the

evaporative cooler at the wet-bulb temperature conditions, as opposed to ambient storage at dry-bulb temperature conditions. The gain in additional postharvest life using passive cooling is remarkable. Even for temperate climates (T_{db} = 20°C and φ_a = 50%), the postharvest life gain is roughly 2-15 days for the fruits considered. However, in reality, this wet-bulb temperature will not be reached in an evaporative cooler due to additional heat sources (e.g., radiation) and non-optimal evaporative cooling. The temperature will also not remain constant throughout the day. Therefore these charts represent the best-case scenario.
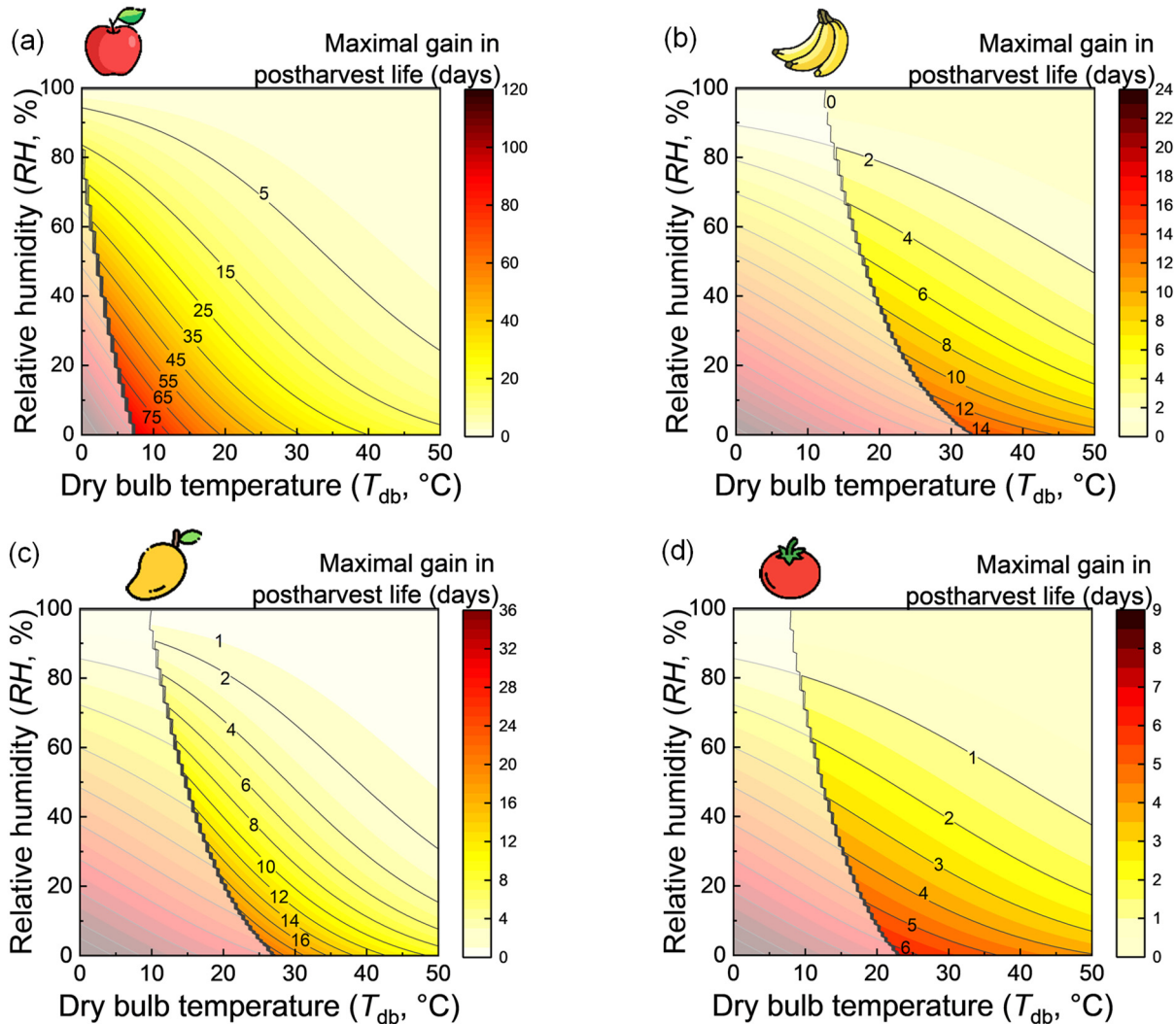
Figure 3. The maximal gain in postharvest life when the wet-bulb temperature is reached as a function of dry-bulb temperature and relative humidity for different fruits: (a) apple, (b) banana, (c) mango, and (d) tomato. The stepped black line indicates the optimal storage temperature for the respective fruit. The postharvest life gain is indicated in translucent coloration for the region where the wet-bulb temperature is above the optimal fruit storage temperature since cooling to temperatures lower than the optimal temperature may be detrimental to the fruit due to chilling injury. This image was created using resources from Flaticon.com.

10

3.2 In which location does it make the most sense to apply evaporative cooling?

We tackle a crucial bottleneck in evaporative cooling here: how to scope for regions where evaporative cooling can be successfully applied (Verploegen, 2021c, 2021b). The evaporative cooling potential and its impact on extending the postharvest life of fresh food at a certain location in the world need to be assessed before deploying evaporative cooling. If evaporative cooling is deployed in a region that does not add postharvest life, farmers will cease to use it and lose trust in the technology. Tools exist to qualitatively assess this cooling potential (Verploegen, 2021b). Our design charts can also identify the temperature depression that can be reached for a certain location worldwide. Using our charts, we can select a specific season or month based on the local environmental conditions (Figure 2, Figure 3). We took the next step by calculating and mapping the gain in postharvest life that evaporative cooling gives at every location in India or Nigeria for each month of the year at a resolution of approximately 30 km (section 3.2.1). Furthermore, we developed a similar map for the entire world for four seasons (section 3.2.2).

3.2.1 Evaporative cooling potential for India and Nigeria

Wet-bulb temperature and maximal temperature depression

Figure 4 indicates the monthly climatic parameters relevant for evaporative cooling under shaded conditions in India and Nigeria, namely the dry-bulb temperature and relative humidity. Figure 5 maps the monthly wet-bulb temperature and the maximal temperature depression achieved by evaporative cooling. We zoom into specific regions in Figure 6.

With respect to the climate, Nigeria has a few clear dry months (November to April) within almost the entire country. These months will also likely be preferred to apply evaporative cooling. The temperatures are relatively high throughout the year and throughout the country, except for the elevated region in Plateau and Adamawa states. In India, a few drier months are present (February to May), mainly in the country's northwestern part. The Himalayas cause a very low-temperature zone in the north of the country.

The maximal temperature depression that can be reached is representative of the gain in postharvest life that we can achieve by evaporative cooling. This depression is the criteria to define the evaporative cooling potential and not the wet-bulb temperature. The temperature depression is strongly correlated with seasonal humidity. We get the highest potential for evaporative cooling in Nigeria between November to April and in India between April and May. In Nigeria, a significant temperature reduction by evaporative cooling can be achieved throughout almost the entire country, except for the coastal region. In India, the largest temperature depression is obtained in the northwestern states (e.g., Gujarat). Here, temperature depressions from ambient, up to 14 degrees Celcius, can be reached due to evaporative cooling. In many states in India and Nigeria, it is too humid to have a significant temperature reduction (higher than 5 °C) by evaporative cooling. In summary, the highest potential locations to apply evaporative cooling are: (1) for Nigeria, the northern states (Sokoto, Kebbi, Borno, and Yobe) in March and April, and (2) for India, Gujarat, and Madhya Pradesh in April and May.

The wet-bulb temperature is also an important parameter, in addition to the maximal temperature depression. It is the lowest storage temperature for fruit and vegetables that can be achieved by evaporative cooling. This produce storage temperature is still relatively high in India and Nigeria in most regions and months that have the highest potential for evaporative cooling. For India and Nigeria, these temperatures are above about 15 °C, so higher than the ideal storage temperatures of most fruits. Therefore, some foods cannot be stored at their optimal temperature with evaporative cooling in these countries. However, a clear reduction of several degrees Celsius can still be obtained when stored in an evaporative cooler at the right location in the country and in the right months. In addition, the higher humidity in the cooler will also help preserve the fruit significantly longer.
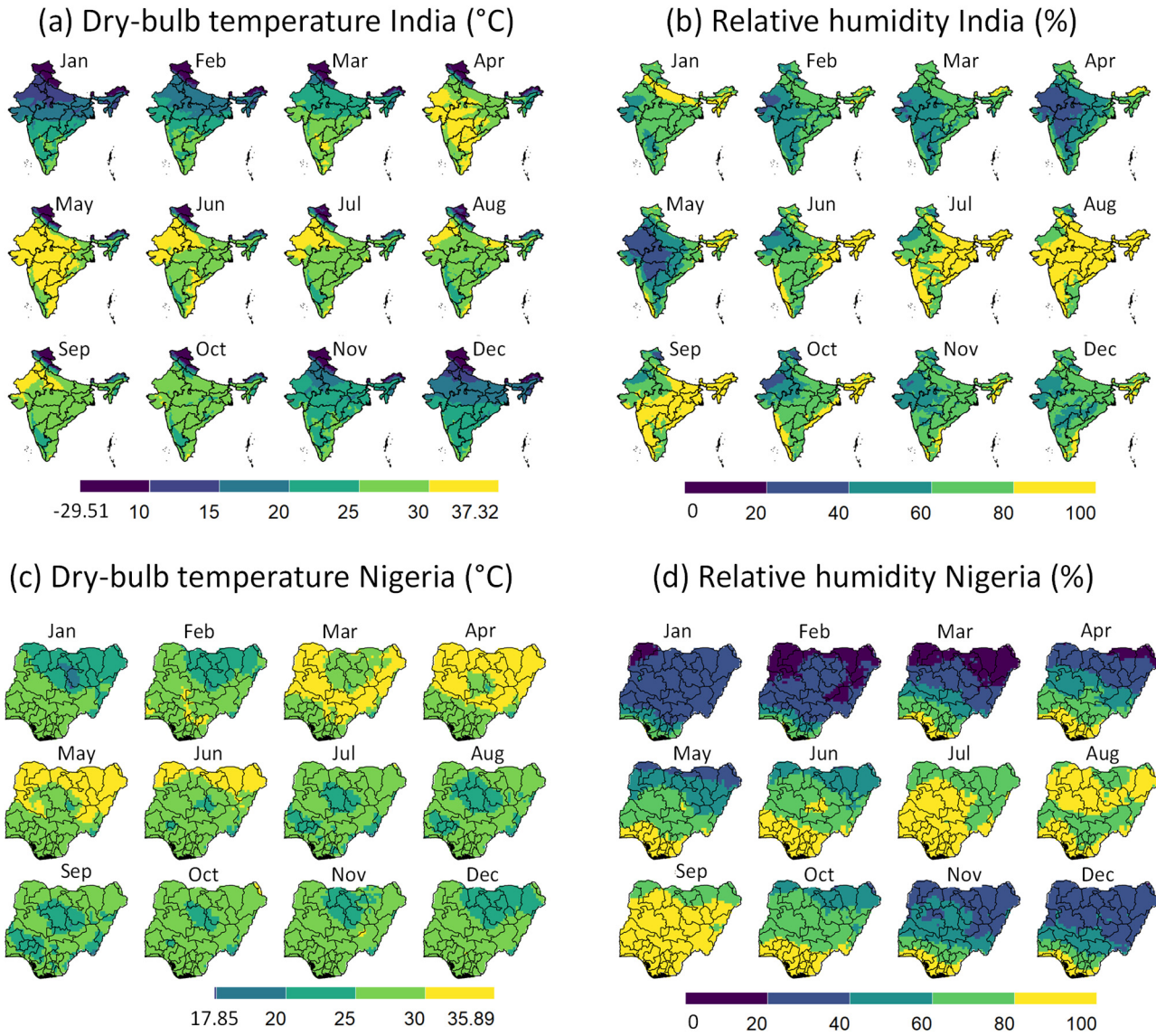
Figure 4. Measured data on the local climate in India, namely the dry-bulb temperature (a) and relative humidity (b) for each month in 2020.
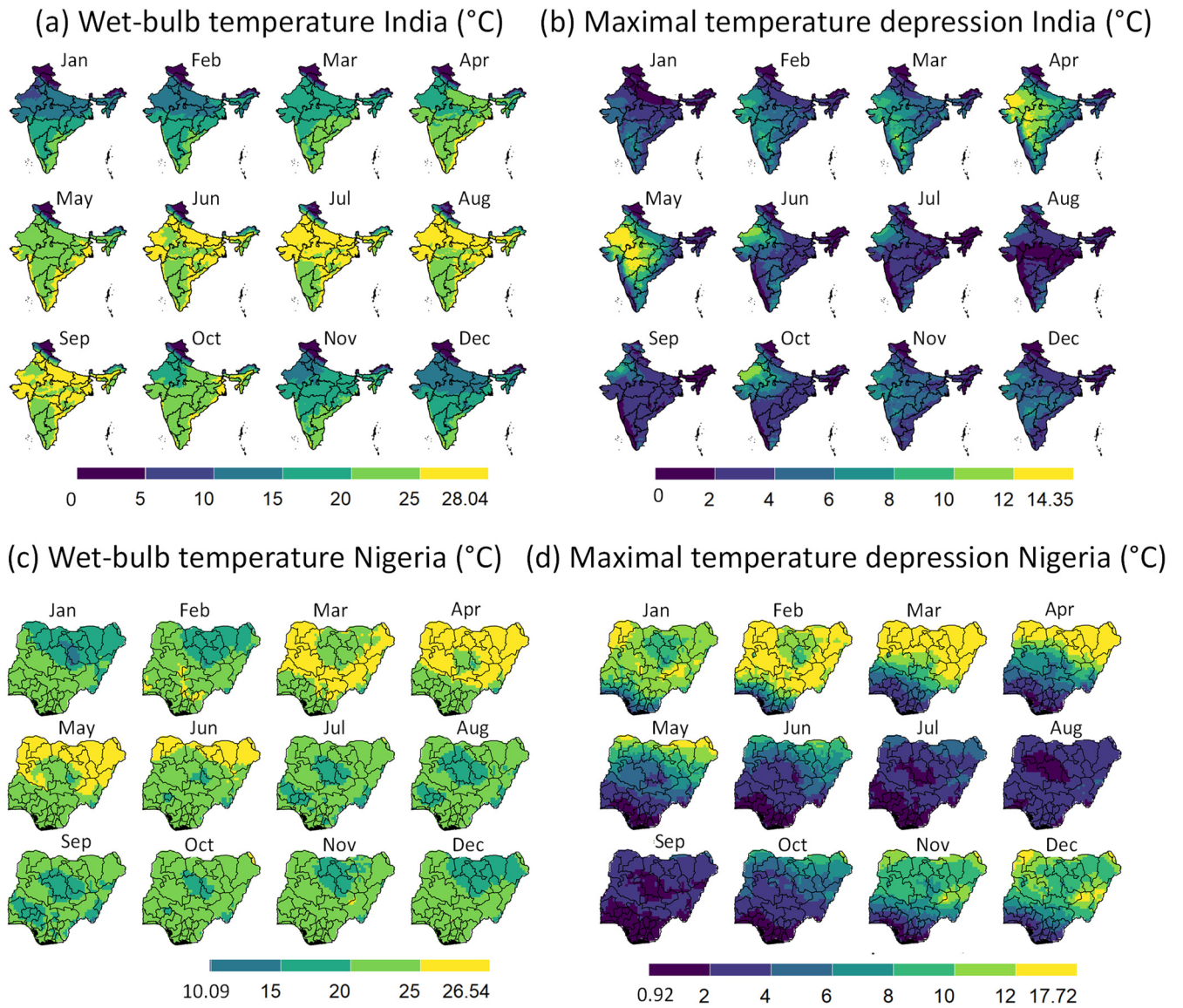
Figure 5. Monthly wet-bulb temperature (a,c) and the maximal temperature depression due to evaporative cooling (b,d) in India (a,b) and Nigeria (c,d), showing the example of 2020.

(a) India, with a focus on the state Gujarat
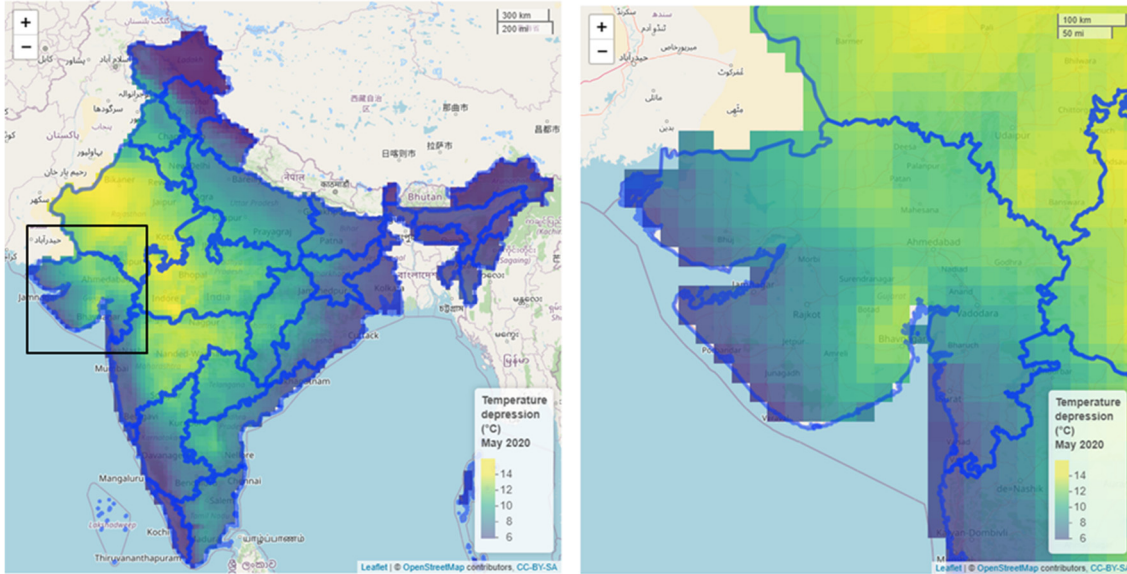
(b) Nigeria, with a focus on the state Plateau
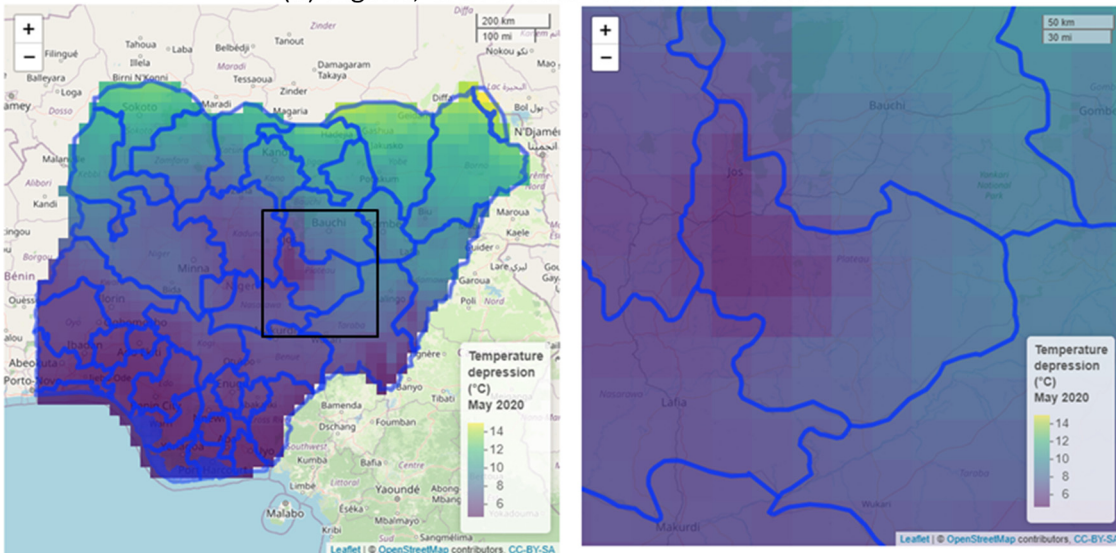
Figure 6. Focus of the maximal temperature depression due to evaporative cooling in Gujarat state in India (a) and Plateau state in Nigeria (b) in May 2020. The pixels have a 30 kilometer resolution.

Gain in postharvest life in an evaporative cooler

Figure 7 illustrates the graphical workflow on how the maximal gain in postharvest life in an evaporative cooler is determined. Here we compared to storing fruit at ambient conditions, calculated from the climatic parameters. We illustrated this workflow for banana fruit for a certain month in India. In Figure 8, we show the maximal postharvest life in each month that can be achieved by storing banana fruit in an evaporative cooler in India, so under wet-bulb conditions (similar to Figure 7d). In

Figure 9, we show the postharvest life gain (Figure 7e) that can be achieved by storing banana fruit in an evaporative cooler (Figure 7d), compared to at ambient in the shade (Figure 7c). These data indicate where there is the highest potential for reducing the temperature and increasing postharvest life by evaporative cooling in India. We filtered these maps for different states in India with the harvest season for a banana crop (Figure 10). Note that there are regions where evaporative cooling does not add additional postharvest life in these maps since the exterior temperature when stored in the shade, is already at or below the optimal storage temperature for the fruit of interest. In case the storage temperature in the evaporative cooler fell below the optimal fruit storage temperature, we used this optimal storage temperature for postharvest life calculations.

14

The gain in postharvest life by placing the products in an evaporative cooler is substantial. Up to 7 days can be gained for banana, for example. We can thus gain a lot of postharvest life days, so reduce food loss by placing fruit in an evaporative cooler. In a related study (Chopra et al., 2022), the gain in days of storage life was quantified for an entire year for leafy amaranth in India similarly. Filtering our results with the harvesting season proved useful to only target those states where evaporative cooling has a large impact at a certain period of the year.
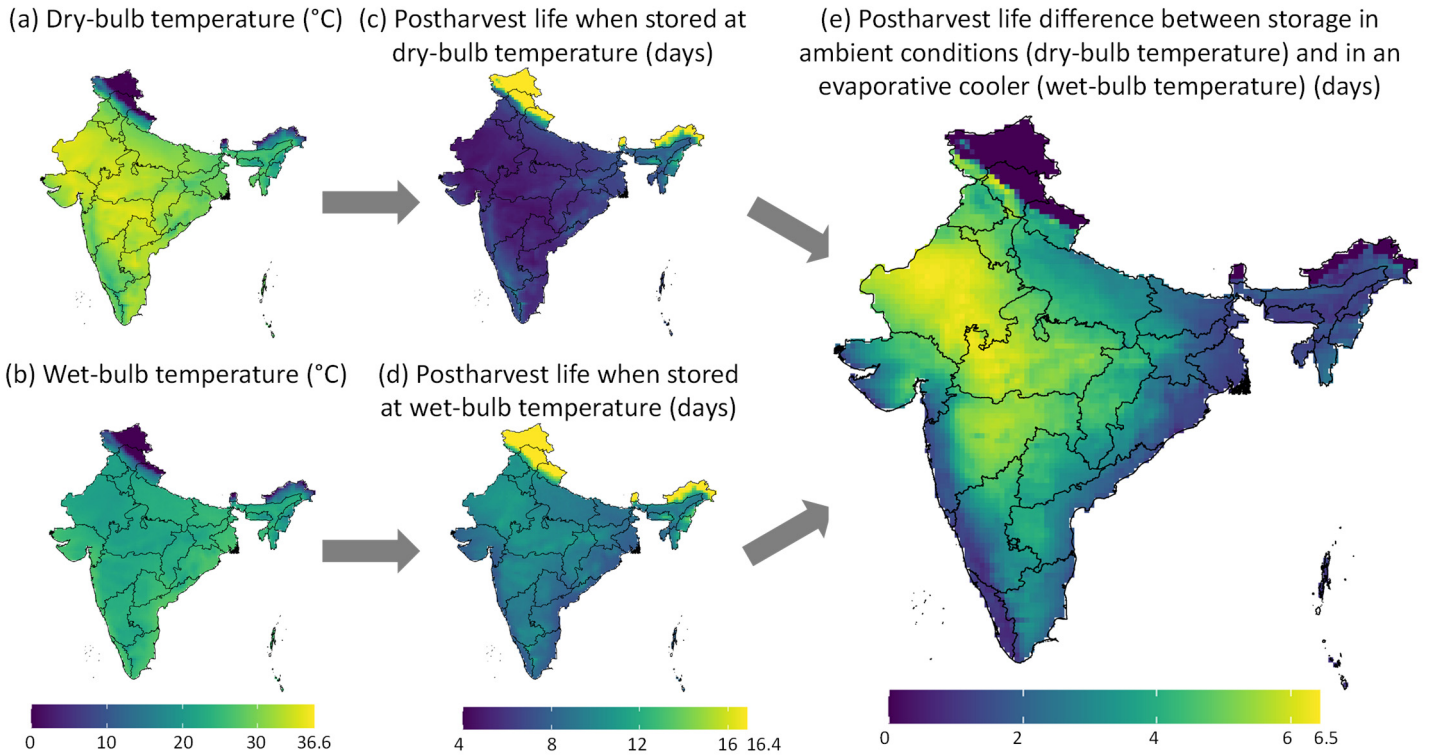
Figure 7. Calculation of the maximal postharvest life in an evaporative cooler calculated from the climatic parameters for banana fruit, showing the example of May 2020. We start from the dry-bulb temperature (a) and wet-bulb temperature (b) to calculate the postharvest life in days (c-d) and then the difference in postharvest life (e).
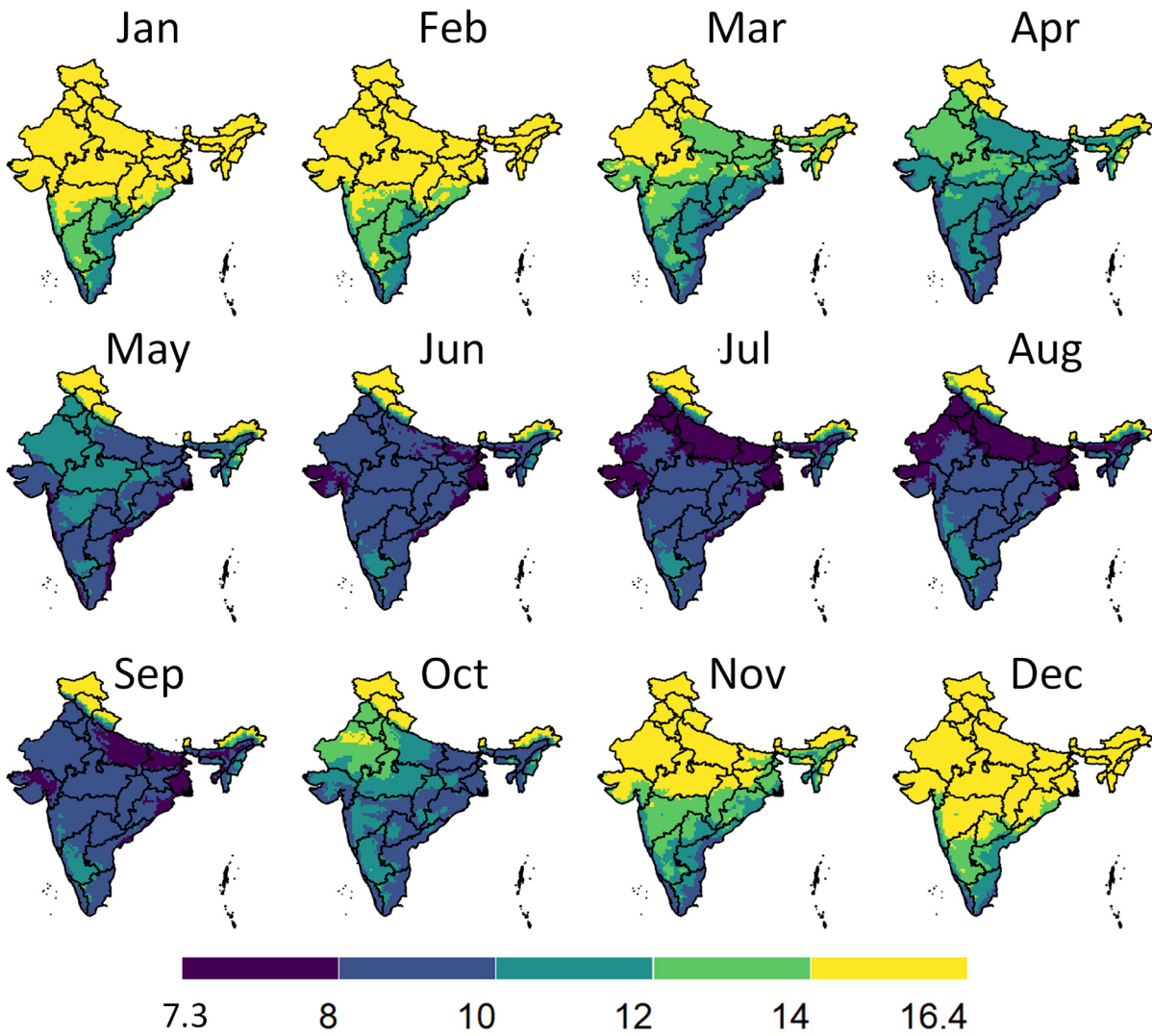
Figure 8. Postharvest life in days in an evaporative cooler for each month for banana fruit in India, so when stored at wet-bulb temperature conditions.
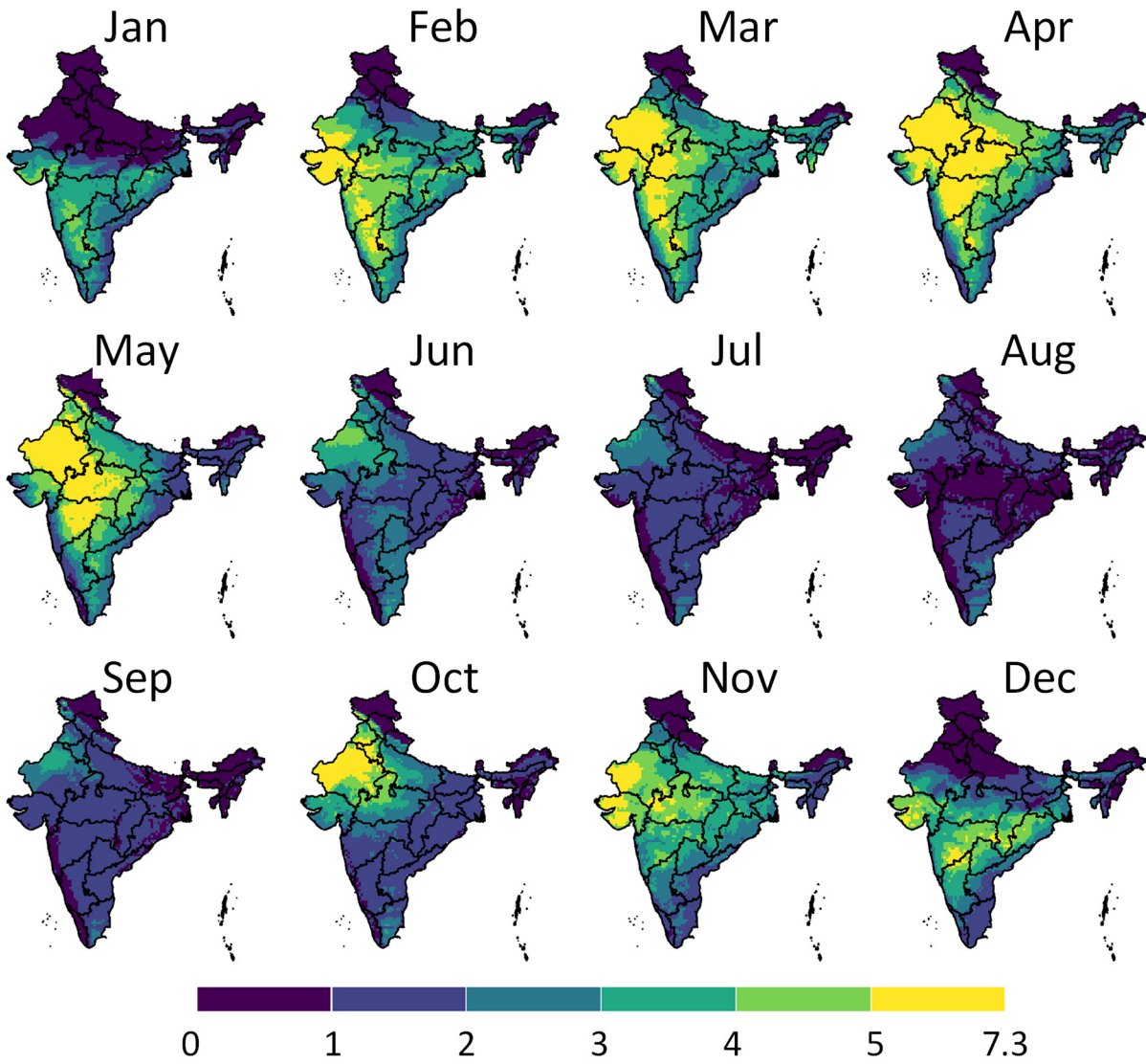
Figure 9. The maximal potential gain in the postharvest life in each month that can be achieved by storing banana fruit in India in an evaporative cooler compared to at ambient temperatures in the shade.

(a) Harvest season
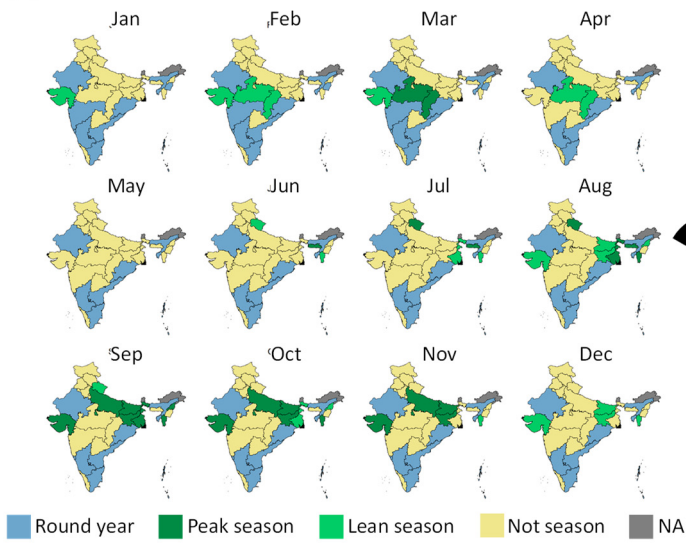
(c) Maximal postharvest life gain in an evaporative cooler (days), filtered with the harvest season

(b) Maximal postharvest life gain by evaporative cooling
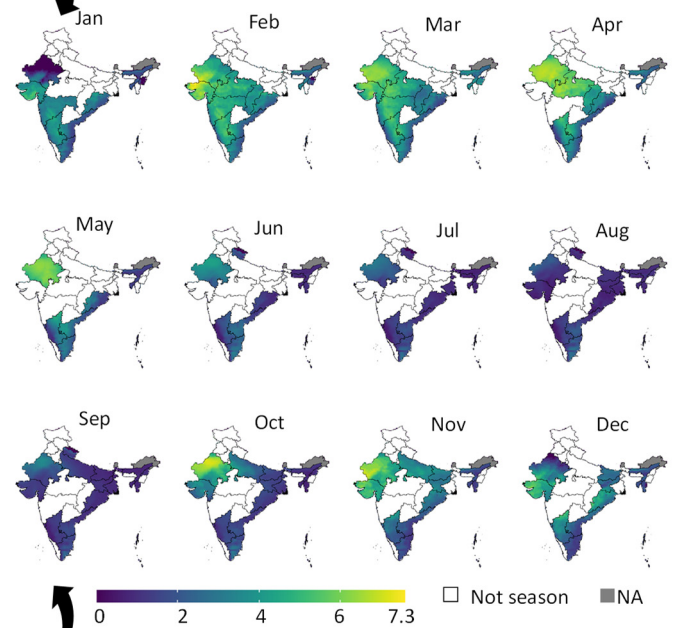
Figure 10. Filtering the maximal postharvest life gain by evaporative cooling for banana (b) with the harvest seasons (a) in each state of India. We obtain the maximal postharvest life difference between storage in ambient conditions (dry-bulb temperature) and in an evaporative cooler (wet-bulb temperature) (days), filtered with the harvest season. The harvest season information was obtained from (Ministery of Commerce & Industry, 2022)**.**

From Figure 11, these regions where the highest evaporative cooling can be achieved for fresh produce also agree to the regions where evaporative cooling is interesting to use for building ventilation in India to improve thermal comfort. A study on 60 cities in India (Hindoliya and Mullick, 2006) quantified in which cities it would make the most sense to use evaporative cooling. The aim was to lower the air temperatures while not increasing the humidity too much to improve the thermal comfort of the people. This study did not consider the efficiency of evaporative cooling but rather identified zones with high ambient temperatures throughout the year and the appropriate relative humidity. If we compare our postharvest life gain map with the one for building ventilation potential (Figure 11), we see a lot of parallels.

18

(a) Shelf life difference between storage in ambient conditions and in an evaporative cooler (days)

(b) Climatic zones indicating potential of direct evaporative cooling in India.
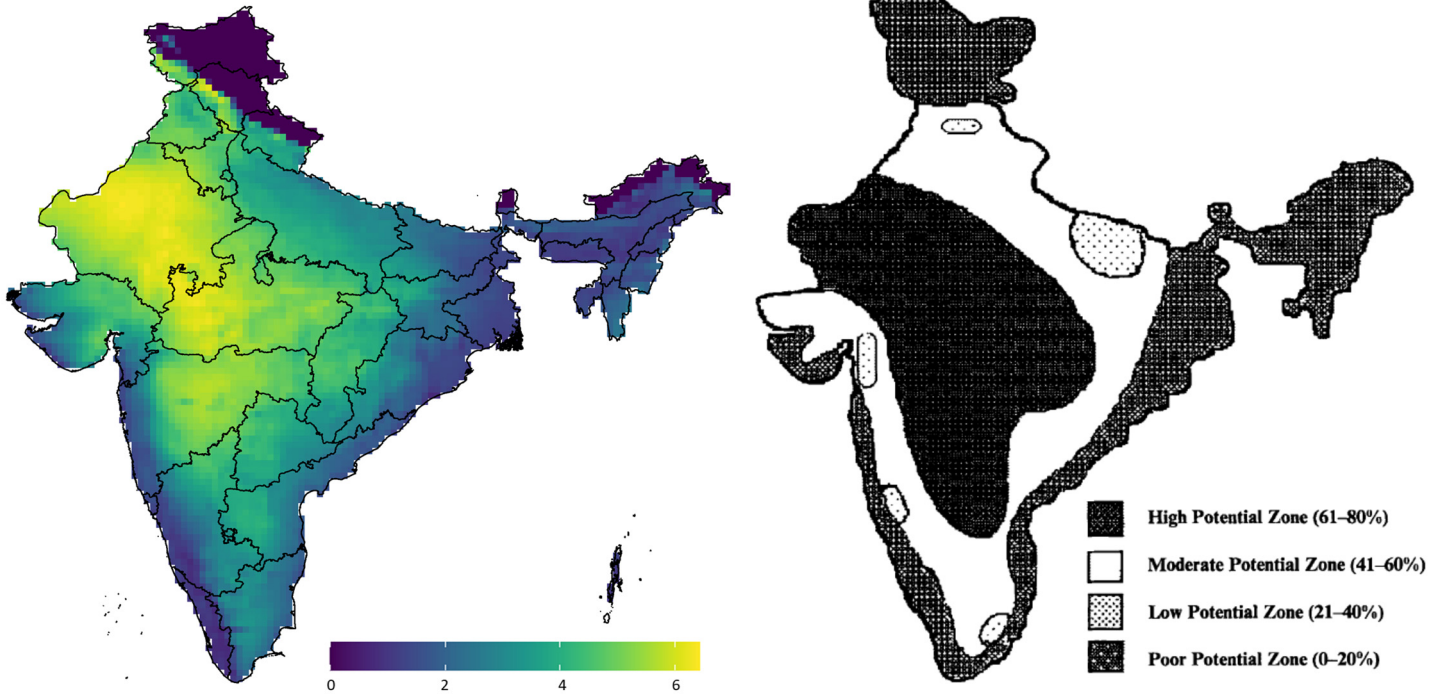
Figure 11. (a) Maximal gain in postharvest life by evaporative cooling for banana, showing the example of May 2020. (b) Climatic zones indicating the potential of direct evaporative cooling in India for the entire year from (Hindoliya and Mullick, 2006)*.*

3.2.2 Evaporative cooling potential for evaporative cooling for the world

In addition to India and Nigeria, we also mapped the temperature reduction potential by evaporative cooling for the entire world for May 2020 (Figure 12) as well as for four months representing four different seasons (Figure 13). This map clearly shows that the potential and effectiveness of evaporative cooling are strongly dependent on the location and the season in which it is applied. These maps are made openly accessible online ((Empa, 2022), https://empasimbiosys.github.io/evapo_cooling_map/). More details are found in the supplementary material.

Note that other researchers have made similar maps to quantify heat exposure and stress of humans, and the impact of loss in working hours, as driven by climate change (Hyatt et al., 2010; Kjellstrom et al., 2018). Here, the computation of their wet-bulb globe temperature and the loss in productivity hours parallels our study's approach.
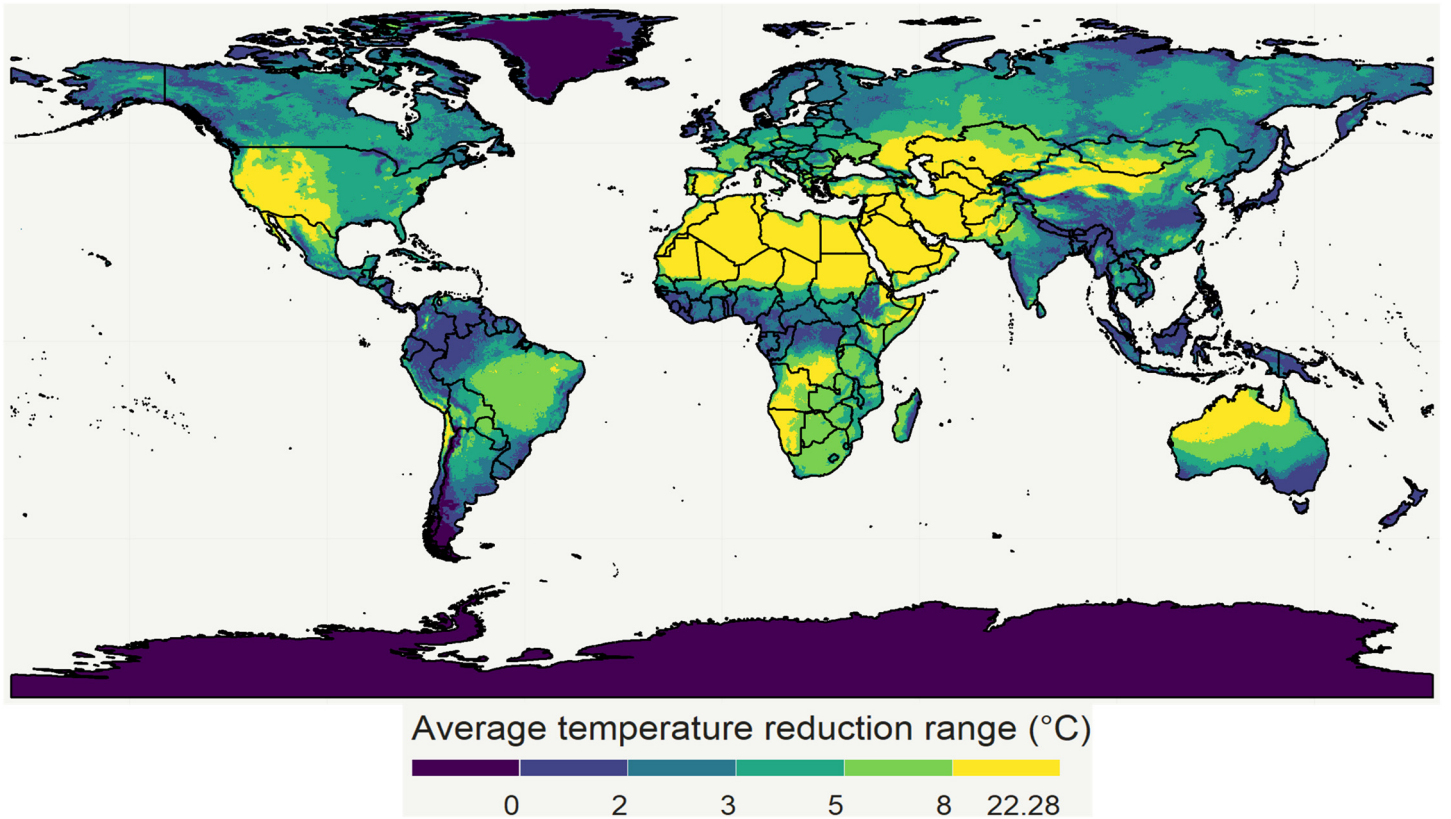
Figure 12. The maximal temperature depression due to evaporative cooling for May 2020. The division of the color scales is based on percentiles of all the 2020 monthly average temperature depression data points. 20, 40, 60, and 80 percentiles correspond to 2, 3, 5, and 8 °C, respectively.
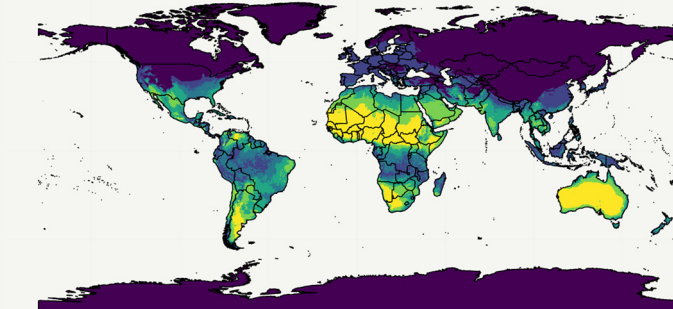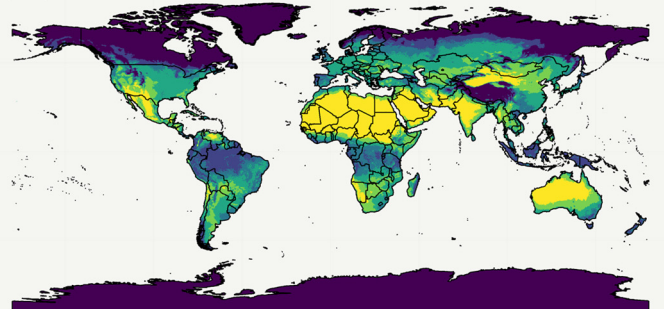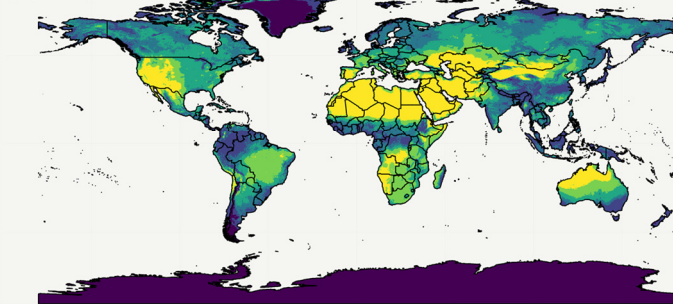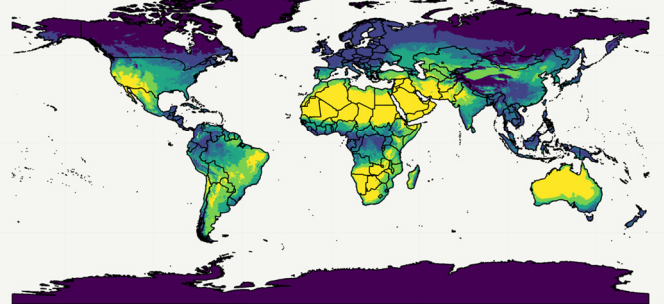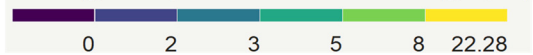
Figure 13. The maximal temperature depression due to evaporative cooling for 4 seasons. The division of the color scales is based on percentiles of all the 2020 monthly average temperature depression data points. 20, 40, 60, and 80 percentiles correspond to 2, 3, 5, and 8 °C, respectively.

3.3   How much fruit can 1 liter of water cool by evaporation?

We aim to quantify how much fruit we can cool with one liter of water by evaporative cooling. This resulting amount of fruit is depicted in Figure 14 as a function of the dry-bulb temperature and relative humidity for apple fruit. In addition, results for mango, tomato, and banana fruit are also shown on the right-hand side, but the differences were very small.

One liter of water can cool down a considerable amount of fruit to the wet-bulb temperature. Note, however, that the wet-bulb temperature might not always be the optimal storage temperature for the fruit. Let us consider a temperature reduction of about 10 °C from the dry-bulb temperature to the wet-bulb temperature. This temperature reduction is achievable by evaporative cooling (Figure 2). Typical conditions in which the wet-bulb temperature drops by 10 °C are, for example, a dry-bulb temperature of about 30 °C and relative humidity of about 40%. When we apply Eq.(7), one liter (or kg) of water can cool down 66 kg of apple fruit by 10 °C. For the same temperature conditions (T_{db} = 30 °C and φ_a = 40%), we can cool down 71 kg of banana fruit, 68 kg of mango fruit, and 62 kg of tomato fruit by 10 °C ideally. Note that these calculations do not consider additional heating by the heat of respiration.

This amount of fruit is the upper limit to which we can cool as we consider a perfect heat extraction from the fruit with no cooling of the air and no additional heat losses. Even if the cooling potential of this one liter of water is lower due to these additional losses, the evaporative cooling capacity of water is huge. One liter of water can easily cool down over tenfold of its weight in fruit by 10 °C.
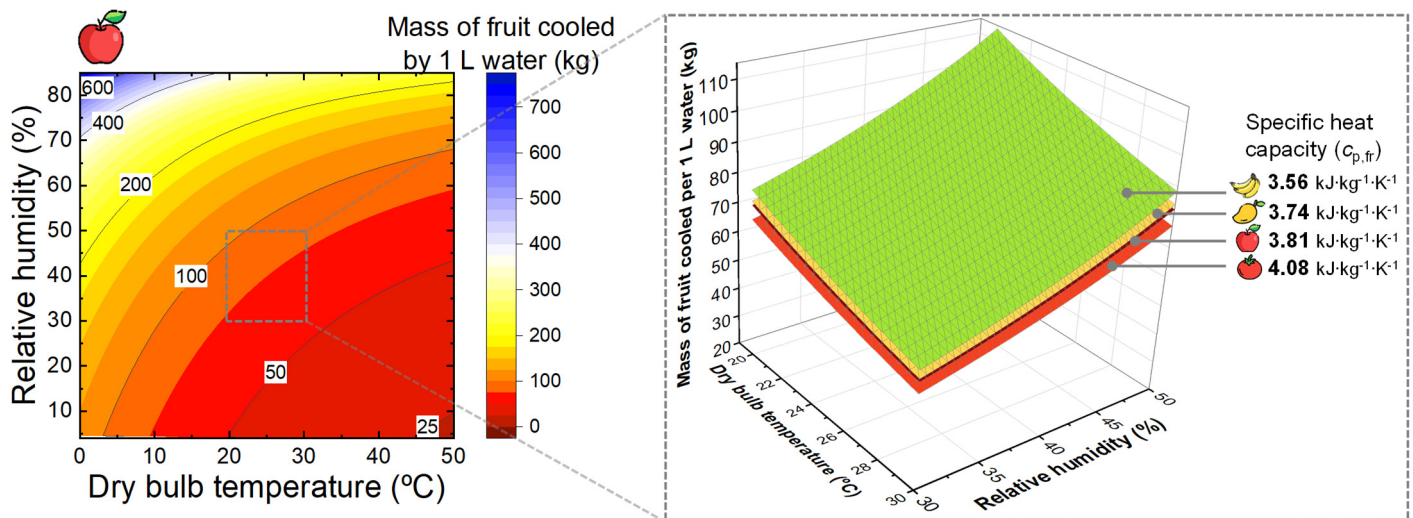
Figure 14. Amount of apple fruit [kg] that one liter of water can cool by evaporative cooling down to the wet-bulb temperature as a function of the environmental conditions where the cooling takes place, namely the dry-bulb temperature and the humidity of the air. The inset on the right shows the effect of the specific heat capacity of fruit for apple, banana, mango, and tomato fruit. This image was created using resources from Flaticon.com.

3.4 **What is the cooling power of an evaporative cooler?**

We aim to quantify the cooling power of an evaporative cooler. We quantify it for a unit cell of a wall of the cooler, so one square meter. We quantify the average cooling power for this unit cell over a specific time. The unit cell is based on our measurements of the charcoal properties and the charcoal cooler we developed previously (Defraeye et al., 2022). We quantified this average cooling power in Figure 15 as a function of the period over which this water is evaporated (Δt) and the thickness of the cooler (D_{ec}).

Larger time intervals for cooling rapidly decrease the cooling power of the evaporative cooler (Figure 15a). A cooler with a thicker wall has a higher cooling capacity for the same time interval. For example, for a time of operation of 5 hours, a cooler with a thickness of 20 cm has a two times higher cooling capacity than a cooler with 10 cm walls.

The moisture content of unsaturated charcoal pieces (w_{PM}) varies strongly depending on the wetting time. We investigated the influence of charcoal moisture content on the cooling power. We varied this parameter between 50 kg m^{-3} and 400 kg m^{-3}. Our findings show that the moisture content of charcoal has a large influence on the cooling power, which is logical as more water is available for evaporation (Figure 15c).

A larger macroporosity decreases the cooling capacity of the evaporative cooler (Figure 15b). This is because as the air space between the charcoal pieces (so higher bulk porosity) increases, the bulk moisture content ($w_{PM,ec}$) decreases. In turn, there is a lesser amount of water for available for evaporation, thus a lower cooling capacity. Increasing the thickness of the cooler and reducing the bulk porosity can lead to a higher cooling capacity of the evaporative cooler. When deciding which of these changes in design parameters should be implemented, important factors to consider are the practicability of implementation and the water use efficiency. Thicker cooler walls would require more water to be added. On the other hand, increasing the porosity between the charcoal pieces too much can compromise the structural integrity of the cooler, by which it can become less self-supporting.

In summary, we can reach a cooling power of several hundred to thousand Watts with one square meter of cooler, which is substantial. We only quantified the average cooling capacity over a specific time interval. We can not, however, guarantee that this cooling capacity can be reached as this implies the amount of water can be evaporated in that amount of time. We cannot control the time interval over which the cooling occurs, as this depends on the environmental conditions and the airspeed, among others. Our time frames assume the conditions are such that this amount can be evaporated. Note that this cooling power is not directly transmitted to the product to be cooled. Finally, note that the heat of respiration produced by the fruit can introduce additional heat to be removed. For example, the heat of respiration for bananas is about 55 W tonne^{-1} at 13 °C and 119 W tonne^{-1} at 20 °C (Kader, 1996). Compared to the cooling power of a cooling blanket of several square meters, these amounts are rather small.
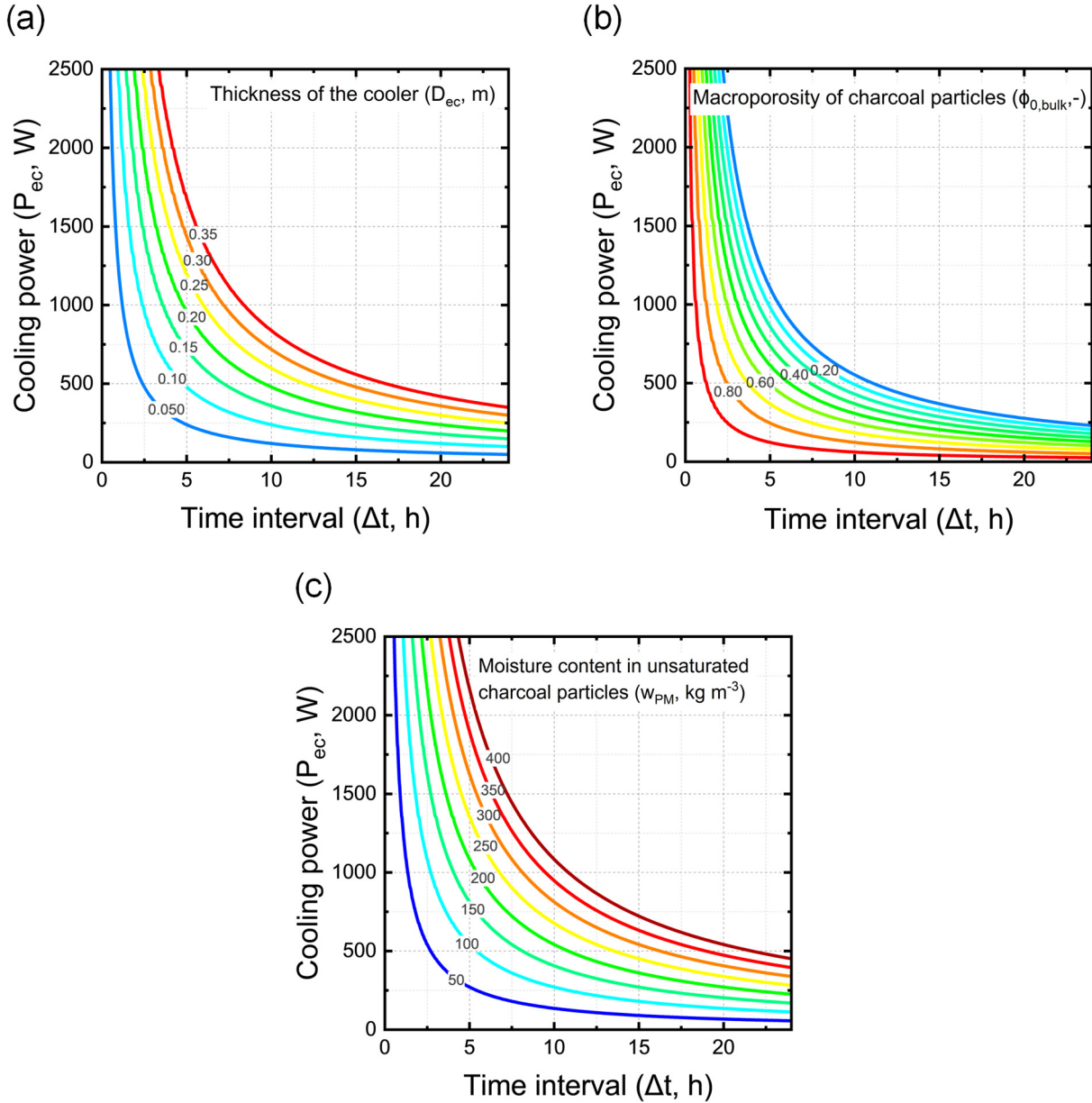
Figure 15. Cooling power of a unit cell wall of an evaporative cooler as a function of the period over which this water is evaporated (Δt) for (a) different thickness of the cooler (D_{ec}) at constant bulk porosity of 61% and moisture content of 88 kg m⁻³, (b) different bulk porosity of charcoal pieces ($\phi_{0,bulk}$) at a thickness of 10 cm and moisture content of 88 kg m⁻³, and (c) different moisture content of charcoal pieces (w_{PM}) at a constant bulk porosity of 61% and thickness of 10 cm.

3.5 How does the airflow rate through an evaporative cooler affect its optimal thickness?

We plot a design chart for calculating the optimal thickness of the walls of the evaporative cooler, given a certain bulk porosity and airspeed (Figure 16). An optimal thickness implies that, under the local airflow conditions at that specific location, the maximal cooling efficiency is reached. The airspeed through the cooler is defined by the local airflow conditions. We assume one square meter of evaporative cooler (A_{ec} = 1 m²) and a spherical charcoal piece size (D_{cc}) of 80 mm. We consider airspeeds ranging between 0.01 and 5 m s⁻¹.

In regions where airspeeds are low and are typically varying during the day around these low values, optimal performance will be difficult to achieve. The reason is that with a slight change of airspeed, the optimal thickness largely varies. As an example, for an evaporative cooler with a bulk porosity of 40% operating in a region with an

23

airspeed of 0.1 m s^{-1}, the optimal blanket thickness would be 76 mm. The optimal blanket thickness would be 350 mm for an evaporative cooler with a bulk porosity of 40% operating in a region with an airspeed of 0.5 m s^{-1}. Once built, we can not change the thickness or bulk porosity so the performance will just vary strongly with airspeed. However, we find that the optimal thickness becomes much more independent of the bulk porosity at higher airspeeds. For example, a 50 mm thick cooler requires about the same bulk porosity for airspeeds above 1 m s^{-1}.

Note that the optimal thickness is independent of T_{db} and φ_a. This implies that the environmental conditions will not determine the required optimal thickness. As such, a cooler with an optimized thickness for specific airflow conditions will perform similarly in different climates.

Such design charts are useful to evaluate for a certain region (country, urban, rural) or locations (free field, building roof) with a certain airspeed how thick the walls of an evaporative (charcoal) coolers should be. This optimal thickness implies optimal efficiency, so the lowest possible temperature and a high cooling capacity. Note that our quantification of the optimal thickness was based on analytical equations. Future steps should be to verify this experimentally or with physics-based simulations. The reason is that the complex transient heat and mass balances cannot be captured fully with simplified analytical equations.
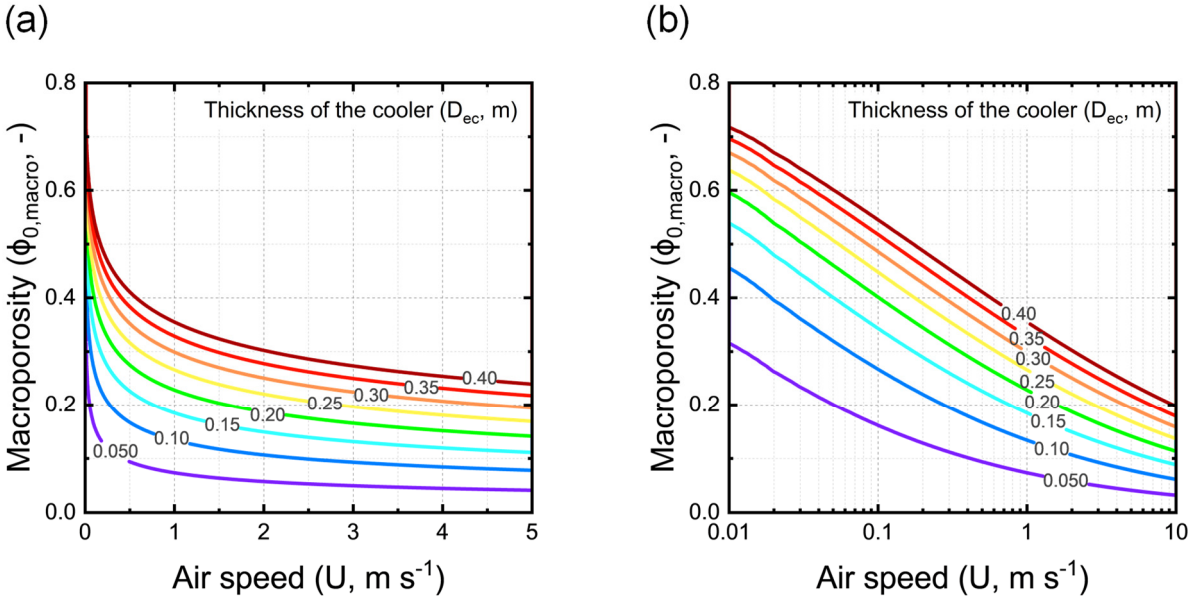
Figure 16. The optimal thickness of the evaporative cooler as a function of the approach flow airspeed (U, m s^{-1}) and bulk porosity ($\phi_{0,bulk}$, -), for charcoal pieces of 80 mm on a (a) linear and (b) logarithmic scale.

4   Conclusions

Evaporative cooling has a huge potential for helping to preserve fresh fruit and vegetables longer after harvest. Single households, smallholder farmers, and farmer cooperatives in developing countries or remote areas benefit especially. However, the extended postharvest life only becomes apparent when the evaporative cooler is used in a location with the right environmental conditions and at the right time of the year to enable sufficient cooling. Our design charts of the temperature depression answer how much evaporative cooling can maximally drop the temperature and extend postharvest life for a certain crop. Mapping this for India, Nigeria, and the entire world quickly targets the best locations and months for evaporative cooling. Such easy-to-use tools are essential during scoping regions for evaporative cooling to avoid disillusions with service providers, policymakers, farmer groups, or cooperatives. Installing evaporative coolers in regions and periods of the year with low potential and disappointing performance are potential causes for farmers' limited adoption of this technology. With the information we present, stakeholders can answer the two most important questions quickly when scoping for evaporative cooling sites: (1) how much can we maximally decrease the fruit storage temperature compared to storing outside under the natural shade, so how much postharvest life can we actually gain here; (2) what is the lowest storage temperature at a specific site and period of the year and how far is this from the ideal storage temperature of that crop.

Once a suitable region is identified, our other design charts enable us to optimally determine the wall thickness of the evaporative cooler based on the local airspeed to have the optimal evaporation rate. Here there is a trade-off between increasing efficiency, so lowering the temperature, and increasing cooling power. However, the target for fresh fruit and vegetables is to maximize temperature drop and humidity levels, not maximizing the cooling capacity.

The information presented in this study aims to catalyze the development of small-scale evaporative coolers. Only then can we make passive postharvest cooling accessible to the currently underserved rural, peri-urban and urban marginal and smallholder farmers. These stakeholders need to see that evaporative coolers bring significant gains in postharvest life, reduce food losses, and increase revenues. They also need to see that evaporative coolers do not perform well in certain locations in their country and certain months of the year. We need to install the coolers only in regions where they help save food and operate them in the most optimal months. Such evidence-based success stories are essential to building trust in this technology. Apart from the farmers, governments, and organizations that disseminate passive cooling technologies, among others, need to be convinced of their potential to communicate to farmers convincingly.

5   Acknowledgments

AUTHOR CONTRIBUTIONS

T.D. conceptualized the study and acquired funding; T.D. did the project administration; T.D., C.S. and K.S. performed the investigation, developed the methodology, and executed the modeling; T.D. wrote the original draft of the paper, with key input from C.S. and K.S.; K.S, and C.S. did the visualization; S.S., D.O. performed critical review and editing.

6 REFERENCES

Allen, R., Pereira, L., Raes, D., Smith, M., 1998. Crop evapotranspiration - Guidelines for computing crop water requirements - FAO Irrigation and drainage paper 56, Evapotranspiración del cultivo Guías para la determinación de los requerimientos de agua de los cultivos. ESTUDIO FAO RIEGO Y DRENAJE 56. Rome.

Allen, R.G., Walter, I.A., Elliott, R.L., Howell, T.A., Itenfisu, D., Jensen, M.E., Snyder, R.L., 2005. The ASCE Standardized Reference Evapotranspiration Equation. ASCE Stand. Ref. Evapotranspiration Equ. 1–203. https://doi.org/10.1061/9780784408056

Ambuko, J., Wanjiru, F., Chemining'wa, G.N., Owino, W.O., Mwachoni, E., 2017. Preservation of Postharvest Quality of Leafy Amaranth (Amaranthus spp.) Vegetables Using Evaporative Cooling. J. Food Qual. 2017, 1–7. https://doi.org/10.1155/2017/5303156

Anyanwu, E.E., 2004. Design and measured performance of a porous evaporative cooler for preservation of fruits and vegetables. Energy Convers. Manag. 45, 2187–2195. https://doi.org/10.1016/j.enconman.2003.10.020

Boettiger, S., Sanghvi, S., 2019. How digital innovation is transforming Indian agriculture | McKinsey, McKinsey & Company report.

Chopra, S., Müller, N., Dhingra, D., Mani, I., Kaushik, T., Kumar, A., Beaudry, R., 2022. A mathematical description of evaporative cooling potential for perishables storage in India. Postharvest Biol. Technol. 183, 111727. https://doi.org/10.1016/j.postharvbio.2021.111727

Dadhich, S.M., Dadhich, H., Verma, R.C., 2008. Comparative study on storage of fruits and vegetables in evaporative cool chamber and in ambient. Int. J. Food Eng. 4, 1–22. https://doi.org/10.2202/1556-3758.1147

Defraeye, T., Schudel, S., Shrivastava, C., Motmans, T., Umani, K., Crenna, E., Shoji, K., Onwude, D., 2022. The charcoal cooling blanket: A scalable, simple, self-supporting evaporative cooling device for preserving fresh foods. engrXiv. https://doi.org/https://engrxiv.org/preprint/view/2221

Elansari, A.M., Yahia, E.M., Siddiqui, W., 2019. Chapter 12 - Storage systems, in: Postharvest Technology of Perishable Horticultural Commodities. Woodhead Publishing, pp. 401–437. https://doi.org/10.1016/B978-0-12-813276-0.00012-2

Empa, 2022. Evaporatieve cooling potential map [WWW Document]. URL https://empasimbiosys.github.io/evapo_cooling_map/

GKI, 2017. Innovating the future of food systems - A global scan for the innovations needed to transform food systems in emerging markets by 2035.

Goedde, L., Ooko-Ombaka, A., Pais, G., 2019. Winning in Africa's Agricultural Market, McKinsey & Company report.

Hindoliya, D.A., Mullick, S.C., 2006. Assessment of utilisation potential of direct evaporative cooling for India. Int. J. Ambient Energy 27, 21–28. https://doi.org/10.1080/01430750.2006.9674998

Hyatt, O.M., Lemke, B., Kjellstrom, T., 2010. Regional maps of occupational heat exposure: past, present, and potential future. Glob. Health Action 3, 5715. https://doi.org/10.3402/gha.v3i0.5715

Jensen, M.E., Burman, R.D., Allen, R.G., 1990. Evapotranspiration and Irrigation Water Requirements. New York.

Kader, A.A., 1996. Fruit Produce Facts - UC Postharvest Technology Center [WWW Document].

Kanali, C., Kituu, G., Mutwiwa, U., Mung'atu, J., Ronoh, E., Njuguna, S., Kamwere, M., Mulamu, L., 2017. RE4Food Project: Energy Efficient Rural Food Processing Utilising Renewable Energy to Improve Rural Livelihoods in Kenya.

Kjellstrom, T., Freyberg, C., Lemke, B., Otto, M., Briggs, D., 2018. Estimating population heat exposure and impacts on working people in conjunction with climate change. Int. J. Biometeorol. 62, 291–306. https://doi.org/10.1007/s00484-017-1407-0

Ministery of Commerce & Industry, G. of I., 2022. Harvesting season of banana [WWW Document]. URL https://apeda.gov.in/apedawebsite/six_head_product/Harvesting_Season_Banana.htm

Mujuka, E., Ambuko, P.J., Mburu, P.J., Ogutu, P.A., 2021. Investment in Technologies : Key Strategy for Postharvest Loss Reduction 2, 47–48.

Ogawa, A., 2021. Psychrometric chart at sea level in SI units [WWW Document]. URL https://commons.wikimedia.org/wiki/File:PsychrometricChart-SeaLevel-SI.jpg

Patel, N., Mindhe, O., Lonkar, M., Naikare, D., Pawar, S, Bhojwani, V.K., Pawar, Sachin, 2021. Performance Investigation of Mitticool Refrigerator, in: Techno-Societal 2020. Springer, pp. 1051–1061.

Rehman, D., McGarrigle, E., Glicksman, L., Verploegen, E., 2020. A heat and mass transport model of clay pot evaporative coolers for vegetable storage. Int. J. Heat Mass Transf. 162, 120270. https://doi.org/10.1016/j.ijheatmasstransfer.2020.120270

Ricciardi, V., Ramankutty, N., Mehrabi, Z., Jarvis, L., Chookolingo, B., 2018. How much of the world's food do smallholders produce? Glob. Food Sec. 17, 64–72. https://doi.org/10.1016/j.gfs.2018.05.002

Robertson, G.L., 2016. Food Packaging: Principles and Practice, Third Edit. ed. Taylor & Francis Group LLC, Boca-Raton. https://doi.org/10.1177/0340035206070163

Sadeghi, S.H., Peters, T.R., Cobos, D.R., Loescher, H.W., Campbell, C.S., 2013. Direct Calculation of Thermodynamic Wet-Bulb Temperature as a Function of Pressure and Elevation. J. Atmos. Ocean. Technol. 30, 1757–1765. https://doi.org/10.1175/JTECH-D-12-00191.1

Shitanda, D., Oluoch, O.K., Pascall, A.M., 2011. Performance evaluation of a medium size charcoal cooler installed in the field for temporary storage of horticultural produce. Agric. Eng. Int. CIGR J. 13, 1–8.

Simões-Moreira, J.R., 1999. A thermodynamic formulation of the psychrometer constant. Meas. Sci. Technol 10, 302–311.

Stull, R., 2011. Wet-bulb temperature from relative humidity and air temperature. J. Appl. Meteorol. Climatol. 50, 2267–2269. https://doi.org/10.1175/JAMC-D-11-0143.1

Teutsch, B., Kitinoja, L., 2019. 100 under 100$ - Tools for reducing postharvest losses. The Postharvest Education Foundation.

Vanndy, M., Buntong, B., Chanthasombath, T., Sanatem, K., Acedo Jr., A., Weinberger, K., 2008. Evaporative Cooling Storage of Tomato in Cambodia and Laos. Acta Hortic. 565–570. https://doi.org/10.17660/actahortic.2008.804.83

Verploegen, E., 2021a. Affordable, Scalable, Overlooked: Evaporative Cooling Can Fight Food Loss – Why isn't the Development Sector Embracing It? [WWW Document]. URL https://d-lab.mit.edu/news-blog/blog/affordable-scalable-overlooked-evaporative-cooling-can-fight-food-loss-why-isnt

Verploegen, E., 2021b. Evaporative Cooling for Vegetable Preservation [WWW Document]. URL https://d-lab.mit.edu/research/evaporative-cooling-vegetable-preservation

Verploegen, E., 2021c. Determining if evaporative cooling has the potential to provide value in a specific context [WWW Document]. URL https://d-lab.mit.edu/research/food/evaporative-cooling-vegetable-preservation/suitability-scoping